
CURVELET-BASED MODEL FOR THE GENERATION OF ANISOTROPIC FRACTIONAL BROWNIAN FIELDS

A PREPRINT

Marcos V. C. Henriques

Departamento de Ciências Exatas e Tecnologia da Informação
Universidade Federal Rural do Semi-Árido
Angicos, Brazil
viniciuscandido@ufersa.edu.br

October 6, 2022

ABSTRACT

We propose a curvelet-based model for the generation of Anisotropic Fractional Brownian Fields, that are suited to model systems with orientation-dependent self-similar properties. The synthesis procedure consists of generating coefficients in the curvelet space with zero-mean Gaussian distribution. This approach allows the representation of natural systems having stochastic behavior in some degree and also obeying to a given angular distribution of correlations. Examples of such systems are found in heterogeneous geological structures, in anisotropic materials and in complex disordered media.

Keywords curvelets · fractional brownian motion · fractal models

1 Introduction

Systems with strong anisotropic properties are very frequent in nature, but unfortunately they present serious difficulties in their characterization and mathematical description. This is the case of complex systems in geology, transport phenomena in material science, wave propagation in disordered media and radiative transfer in systems that do not have a spherical symmetry.

An example with technological application is related to the problem of petroleum exploration. In this problem, the main used technique is related to the phenomenon of scattering of seismic waves in geological structures with anisotropic inhomogeneities in all scales. To take into account the fluctuations of the physical quantities of these structures it is necessary to describe their properties in a statistical way. In these systems, the geological data are best modeled by fractal geometries as the ones created by Mandelbrot [Mandelbrot and Van Ness(1968)]. For example, it has been reported by several authors that well log data from petroleum reservoirs show long-range correlation behavior, which is a characteristic feature of fractal processes like the Fractional Brownian Motion [Hewett(1986), Sahimi and Tajer(2005), Dashtian et al.(2011)Dashtian, Jafari, Sahimi, and Masihi, Hardy and Beier(1994)]. It has been also reported [Hansen et al.(2011)Hansen, Lucena, and Da Silva] that long range correlations in unconsolidated sandstones and porous media can be understood as the consequence of extreme dynamics restructuring processes occurred during the geological evolution. The onset of anisotropy in these geological systems can be related to the influence of the gravitational field and to macroscopic material flows. Characterizing long-range correlations in these systems, such as porous media described by the porosity logs, may prove useful for an accurate interpretation of geological data.

When analysing layered rocks and geological fields formation due to stratification process, we can verify that geometrical and/or transport properties may be characterized in terms of their anisotropy degree [Sahini and Sahimi(1994), Dullien(2012), Makse et al.(1995)Makse, Davies, Havlin, Ivanov, King, and Stanley]. Indeed, the probability of occurrence of a given porosity (or permeability) gradient is strongly dependent on the orientation of the rock properties. Consequently, these systems are characterized by highly anisotropic correlations. Studies in other areas deal with similar phenomena. For example,

Ponson et al [Ponson et al.(2006)Ponson, Bonamy, Auradou, Mourot, Morel, Bouchaud, Guillot, and Hulin] have studied the self-affine properties of anisotropic fracture surfaces. Jennane et al [Jennane et al.(2001)Jennane, Ohley, Majumdar, and Lemineur] have observed anisotropic correlation in images of bone X-ray tomographic microscopy projections.

Since the early work of Mandelbrot [Mandelbrot and Van Ness(1968)], the Fractional Brownian Motion model (FBM) is largely being used to treat a wide variety of natural phenomena having self-similarity and long-range correlations. In particular, the fractal analysis study applied to bidimensional fields has proved to be very useful to describe some physical properties such as roughness and porosity. However, the standard FBM model is only suitable for describing materials and media that show isotropic symmetry. In that context, generalizations of the FBM to anisotropic models have been proposed in last years. Kamont [Kamont(1995)] studied the Fractional Anisotropic Wiener Field. Bonami and Estrade [Bonami and Estrade(2003)] analysed the properties of various models of anisotropic Gaussian fields and proposed a new procedure to characterize the anisotropy of such fields. Tavares and Lucena [Tavares and Lucena(2003)] and Heneghan [Heneghan et al.(1996)Heneghan, Lowen, and Teich] have implemented wavelet-based models for anisotropic hypersurfaces. Biermé and Richard [Biermé and Richard(2008)] have applied Radon Transform to estimate the anisotropy of Fractional Brownian Fields. Xiao [Xiao(2009)] has studied sample path properties of such anisotropic fields. It will be desirable to generalize these concepts and ideas in simple and automatic ways that can allow sparse representations of highly complex anisotropic fields.

In this paper, we introduce a new method for generating 2-D Anisotropic Fractional Brownian Fields (AFBF) based on the Curvelet Transform. This is a new multiscale transform with strong directional character that provides an optimal representation of objects that have discontinuities along edges [Candes and Donoho(2000), Starck et al.(2002)Starck, Candès, and Donoho, Candès and Donoho(2004)]. The curvelets are localized not only in the spatial domain (location) and frequency domain (scale), but also in angular orientation, which is a step ahead compared to Wavelet Transform [Stephane(1999)]. This directional feature is the one we use to achieve the anisotropy.

2 The Fractional Brownian Motion

We start with the model of Fractional Brownian Motion proposed by Mandelbrot [Mandelbrot and Van Ness(1968)]. An isotropic two-dimensional Fractional Brownian field (FBF) $B_H(u)$, $u \in \mathbb{R}^2$, with Hurst index H taking values in $(0, 1)$, is defined by the correlation function

$$E[B_H(u)B_H(v)] = C_H \left(|u|^{2H} + |v|^{2H} + |u - v|^{2H} \right), \forall u, v \in \mathbb{R}^2, \quad (1)$$

where $E[\cdot]$ is the expectation operator and C_H is a constant depending on H . $B_H(u)$ is not a stationary process, but its increments form a stationary, zero-mean gaussian process, with variance depending only on the distance Δu :

$$E \left[|B_H(u + \Delta u) - B_H(u)|^2 \right] \propto \Delta u^H.$$

It follows from (1) that B_H is a self-similar field:

$$B_H(\lambda u) \stackrel{d}{=} \lambda^H B_H(u),$$

where $\stackrel{d}{=}$ means equal in distribution, and $\lambda > 0$ is a constant. It can be proved that B_H has an average spectral density of the form:

$$S(\xi) \propto |\xi|^{-2H-2} \quad (2)$$

in which $\xi = (\xi_1, \xi_2)$ are the frequency coordinates in the Fourier domain. As proposed in [Bonami and Estrade(2003)], anisotropic fields with stationary increments can be defined by taking orientation-dependent spectral densities of the form:

$$S(\xi) \propto |\xi|^{-2H_\theta-2}$$

where the Hurst index H_θ now depends on the direction of ξ , labeled by the index θ . We consider H a parameter related to the roughness and regularity of the surface. So, in the case of anisotropy, we would expect that H_θ would be related to the self-similarity properties of the field on a given direction. A 1-D process obtained by selecting any straight line of an isotropic FBF B_H is a FBM with Hurst index H . However, contrary to what one would expect, the estimation of the orientation-dependent Hurst index H in an anisotropic Gaussian field cannot be performed simply by analysing sample lines of the field, as in the isotropic case, since the regularity along a line do not appear to be dependent on the direction. In order to measure the anisotropy dependence of Hurst exponent H_θ , Bonami and Strade [Bonami and Estrade(2003)]

developed a procedure, the Directional Average Method (DAM), which consists in computing the average over all the lines orthogonal to θ . The resulting 1-D process, a Fractional Brownian motion (FBM), will have a Hurst index equal to $H_\theta + 1/2$ (in fact, they have proved this to be true for the critical Hölder exponent, which in turn corresponds to the Hurst index in FBM paths [Biermé and Richard(2008)]). We will use a modified version of this procedure later to test accuracy of our curvelet-based method of synthesis.

3 The Curvelet Transform

The Curvelet transform is a recent multiscale analysis developed by Candès and Donoho [Candes and Donoho(2000)]. A curvelet at scale 2^{-j} is an oriented object whose support is the rectangle of width 2^{-j} and length $2^{-j/2}$ that obeys the parabolic scaling relation $width \approx length^2$ [Candes et al.(2006)Candes, Demanet, Donoho, and Ying]. The curvelets are described by a triple index j (scale), l (orientation) and k (spatial location). The basic curvelets elements are obtained by rotations and translations of a specific basis function $\phi_j \in L^2(\mathbb{R}^2)$, called curvelet mother, that depends only on the scale index j and is defined in the Fourier domain by the window function [Candes and Donoho(2000)]:

$$\hat{\phi}_j(r, \omega) = 2^{-3j/4} W(2^{-j}r) V\left(\frac{2^{\lfloor j/2 \rfloor} \omega}{2\pi}\right), \quad (3)$$

where we use the polar coordinates (r, ω) in the Fourier domain, and $\lfloor j/2 \rfloor$ is the integer part of $j/2$. W and V are the “radial window” and the “angular window”, respectively. These two functions are smooth, non-negative and real-value, with W taking positive real arguments. W and V restrict the support $\hat{\phi}_j$ to a polar wedge that is symmetric respect to zero.

Let us define the window $u_{j,l} = \hat{\phi}_j(R_{\theta_{j,l}}\xi)$, where $\xi \in \mathbb{R}^2$ is the cartesian coordinates in the Fourier domain and $R_{\theta_{j,l}}$ is the rotation matrix by $\theta_{j,l}$ radians. The family of curvelets $\phi_{j,l,k}$ is defined in the Fourier domain as:

$$\hat{\phi}_{j,l,k} = u_{j,l} e^{i\langle b_k^{j,l}, \xi \rangle},$$

at scale 2^{-j} , orientation $\theta_{j,l}$, and position $b_k^{j,l} = R_{\theta_{j,l}}^{-1}(2^{-j}k_1, 2^{-j/2}k_2)$, where $k = (k_1, k_2) \in \mathbb{Z}^2$. The curvelet transform of a function $f \in L^2(\mathbb{R}^2)$ is given by the convolution integral:

$$c_{j,l,k} = \langle f, \varphi_{j,l,k} \rangle = \int_{\mathbb{R}^2} f(x) \varphi_{j,l,k}^*(x) dx. \quad (4)$$

where $\bar{\phi}$ denotes the complex conjugate of ϕ . In this equation the coefficients $c_{j,l,k}$ are interpreted as the decomposition of f into a basis of curvelets functions $\varphi_{j,l,k}$ [Candes and Donoho(2005)].

The discrete version of this transform is done by choosing a discrete tiling in the Fourier domain with pseudo-polar supports for the window functions $u_{j,l}$, which is more adapted to cartesian arrays [Candes et al.(2006)Candes, Demanet, Donoho, and Ying]. Figure 1 shows an example of such a discrete curvelet tiling, with each wedge being linked to its corresponding window function $u_{j,l}$. The discrete curvelet transform consists, roughly speaking, in obtaining inner products in the Fourier domain, since, based on Plancherel’s Theorem, we have $c_{j,l,k} = \langle f, \varphi_{j,l,k} \rangle = \langle \hat{f}, \hat{\varphi}_{j,l,k} \rangle$. Therefore we can recover the original signal by using the reconstruction formula

$$f = \sum_{j,l,k} c_{j,l,k} \varphi_{j,l,k} \quad (5)$$

4 The Curvelet-based Model for Anisotropic Fractional Brownian Fields

Wavelet-based methods for synthesis of two-dimensional FBF have been proposed by Tavares [Tavares and Lucena(2003)] and Heneghan et al [Heneghan et al.(1996)Heneghan, Lowen, and Teich]. They show that the wavelet detail coefficients $d_{j,k}$ at scale 2^{-j} of a 2-D FBF with Hurst index H have a zero-mean Gaussian distribution with variance that varies as a power-law in scale with the form:

$$\mathbb{E} \left[|d_{j,k}|^2 \right] = C_H^\psi 2^{-j(2H+2)}, \quad (6)$$

where C_H^ψ is a constant depending on H and the wavelet ψ used, and $k \in \mathbb{Z}^2$ is a index related to spacial location. So, in order to synthesize a 2-D FBF, one has only to generate a series of coefficients with Gaussian distribution and the given variance at each scale, and then transform to the real space.

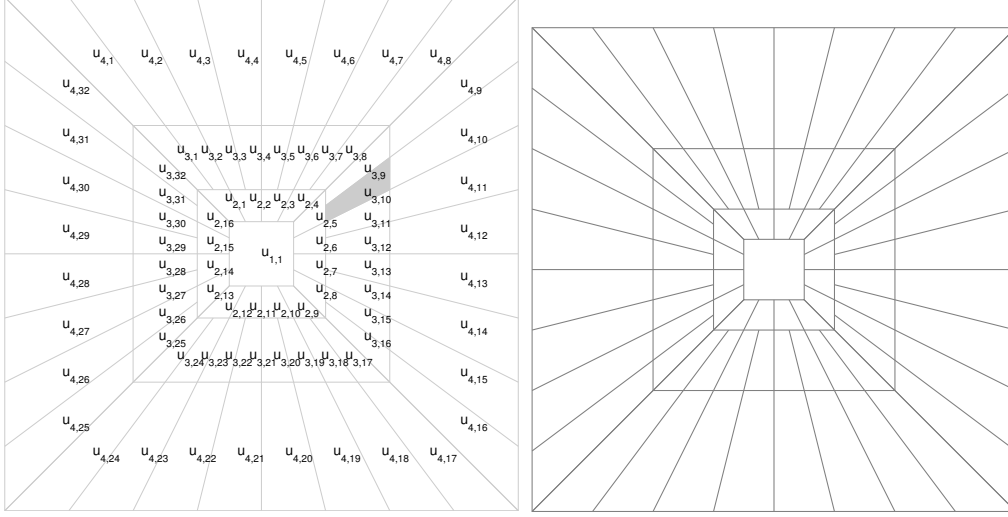


Figure 1: A basic discrete curvelet tiling with the first 4 scales in the Fourier domain. Each $u_{j,l}$ represents a window function at scale 2^{-j} and orientation $\theta_{j,l}$. A sample support for a given window $u_{j,l}$ is marked with gray.

We construct the anisotropic FBF with the curvelet transform in the following way. We introduce an angular variable by dividing the 2π angle of the plane into N identical angular sectors which are identified by a variable m . For each angle index l and scale 2^{-j} , $j > 1$, we generate a matrix of coefficients $c_{j,l,k}$ with zero-mean Gaussian distribution and variance

$$\mathbb{E} \left[|c_{j,l,k}|^2 \right] = C_{H_m}^\phi 2^{-j(2H_m+2)}, \quad (7)$$

where now the Hurst index, H_m , depends on the index $m = 1, 2, \dots, N$, related to the orientation, which in turn is independent of scale and can assume one of the N integer values. For each angular sector there is only one value for m . $C_{H_m}^\phi$ is a constant depending on H_m and on the curvelet ϕ . For practical reasons, we consider $C_{H_m}^\phi = \text{constant}$, independently of m . The relation among m , the curvelet indexes j (scale) and l (scale-dependent orientation) is

$$m = \lceil Nl/n_j \rceil$$

where $\lceil x \rceil$ denotes the smallest integer being greater than or equal to x , and $n_j = 8 \cdot 2^{\lceil j/2 \rceil}$, for $j > 1$, is the number of available angles at the scale 2^{-j} , which is determined by the parameters of the curvelet transform. We have set the first scale $j_0 \equiv 1$ and, by definition, $n_1 \equiv 1$, that is to say, there is no distinct directions at the coarsest scale. We define N to be the number of available angles at second scale ($N \equiv n_2$), since this is the maximum possible number of angular sectors we can split the discrete tiling of frequency space (see figure 2). In our case we use $N = n_2 = 16$, so H_m can assume 16 different values. For heuristic reasons, we have set $H_0 = \mathbb{E}[H_m]$ to be the index associated with the first scale. In figure 2 is shown a sample set of wedges in the Fourier plane associated with a given H_m index.

After generating the coefficients, all we have to do is to perform the inverse curvelet transform as expressed by (5) to get the anisotropic field.

5 Results

Figure 4 shows three synthesized isotropic fractional brownian fields. (a) presents an isotropic field with Hurst index 0.1, (b) presents an isotropic field with Hurst index 0.5 and (c) presents an isotropic field with Hurst index 0.9. Figure 4 shows three simulations of anisotropic fractional brownian fields. The angular distribution of the H_m indexes used in each simulation is shown on top. (a) we see a case with abrupt change of H_m in the angular distribution, from 0.2 around the vertical direction to 0.9 around the horizontal direction. (b) presents an anisotropic field, with Hurst indexes ranging from 0.1 along east direction to 0.9 along north direction. We can see in this example that the generated field seems to have anticorrelation along one axis (east) and correlation along other (north). (c) presents an anisotropic field, with Hurst indexes ranging from 0.1 along a direction almost northwest to 0.9 along almost northeast. At the bottom is shown the logarithm of the power spectrum illustrating the directional character of the synthesized fields.

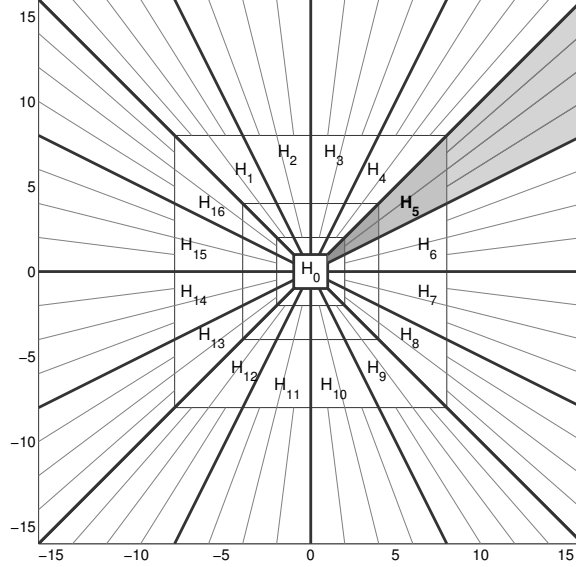


Figure 2: A sample set of wedges in the Fourier plane associated with a given H_m index is marked with gray.

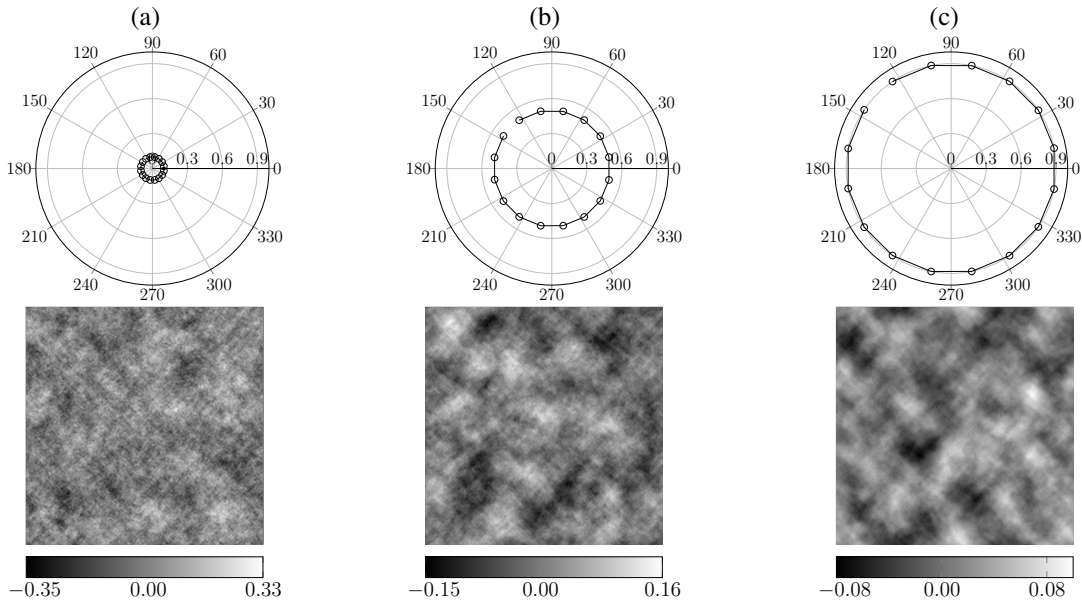


Figure 3: Three examples of isotropic Fractional Brownian Fields obtained by using the curvelet method. Top: the angular distribution of H_m index used in the synthesis of each field. Bottom: the corresponding synthesized fields.

For the evaluation of the quality of our synthesis procedure, we must measure the Hurst index for each direction in the generated field and to compare with the H_m value used in the construction. For this, we apply a modified version of the Directional Average Method (DAM) proposed in [Bonami and Estrade(2003)]. As said before, this method was developed to estimate the orientation-dependent index H in anisotropic Gaussian fields. It consists in obtaining a 1-D signal that is the average over all the lines orthogonal to a given direction θ . The estimated Hurst index of this signal must be about $H_\theta + 1/2$, where H_θ is the desired parameter to characterize the field. In order to get the 1-D signal we proceed as follows. The matrix representing the field is treated as a monochrome image. We rotate this image by θ in a clockwise direction, by using an image processing operator that includes a bicubic interpolation [Keys(1981)], but others methods can also be applied. The output, expressed as a matrix, is large enough to contain the information of the entire rotated image, from which we extract an inscribed submatrix whose columns represent an approximation to the lines orthogonal to θ in the original data. This procedure is illustrated in figure 5. So we can directly get the output 1-D signal by taking the average of each column of this submatrix. Finally, we estimate the Hurst index of the signal by

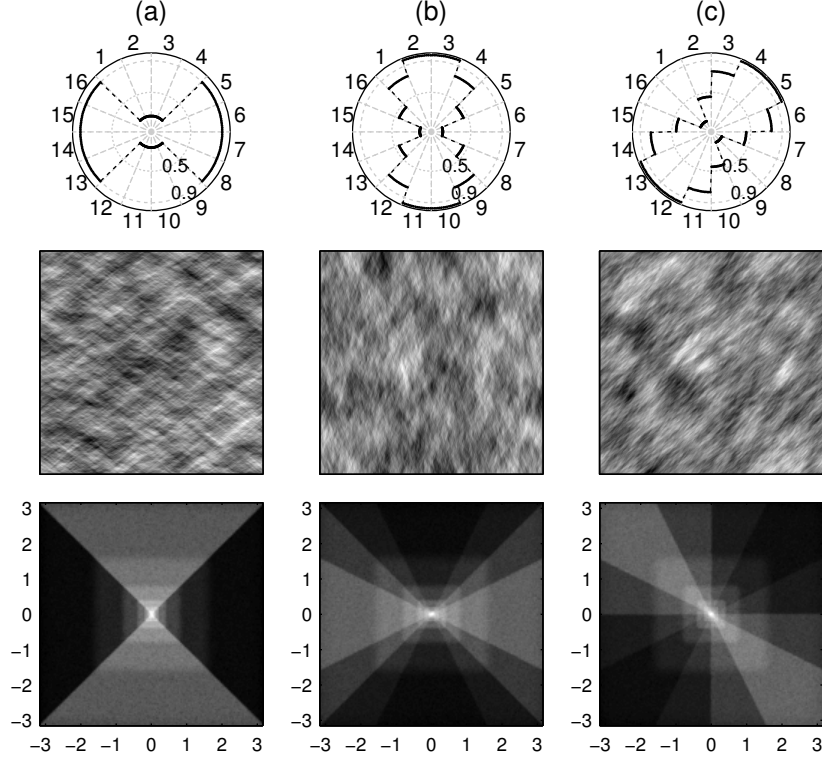


Figure 4: Three examples of anisotropic Fractional Brownian Fields obtained by using the curvelet method. Top: the angular distribution of H_m index used in the synthesis of each field. Middle: the corresponding synthesized fields. Bottom: The corresponding spectral density.

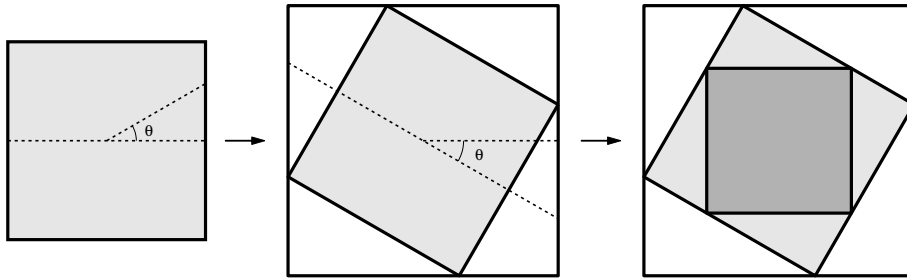


Figure 5: Scheme of rotation of the image that represents the field.

using a method of choice. This process is performed, in our case, for each one of the N angles used in the synthesis by curvelets.

Figure 6 shows the mean of the estimated Hurst parameters at 16 directions of 50 generated samples with 2000×2000 points. Three methods of FBM analysis were used. The first one, proposed by Peng et al [Peng et al.(1994)Peng, Buldyrev, Havlin, Simons, Stanley, and Goldberger], uses Detrended Fluctuation Analysis (DFA) to estimate H . The others two, periodogram method and boxed periodogram method, use the observation that the spectral density of a FBM behaves like (2). For details of these last two methods we refer to [Taqqu et al.(1995)Taqqu, Teverovsky, and Willinger]. The FBM analysis method that gives smaller mean squared error is the DFA-based method, as shown in the figure.

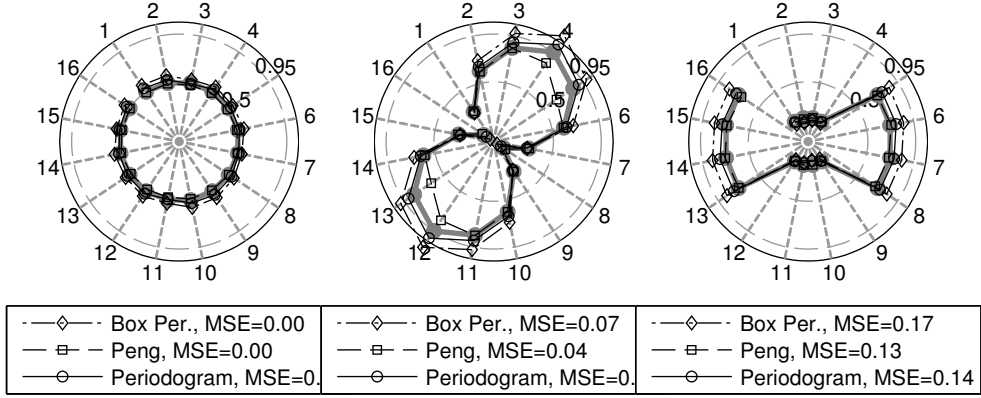


Figure 6: Anisotropy analysis by the Directional Average Method (DAM) of 50 samples with 2000×2000 points. (MSE= Mean Squared Error)

6 Final Remarks

We have proposed a curvelet-based scheme for generating Anisotropic Fractional Brownian Fields with orientation-dependent self-similar properties. It can create surfaces with an arbitrary angular distribution of Hurst parameters, which is a step forward with respect to wavelet-based approaches such as Tavares and Lucena method [Tavares and Lucena(2003)]. Our proposed algorithm gives good results even in case of abrupt change of the orientation-dependent Hurst index H_m in the angular distribution.

We expect this method to be useful in the study of systems where long-range dependent stochastic processes arise, as for example, in geostatistics of large scale anisotropic porous media. All we have to do is to generate curvelet coefficients with zero-mean Gaussian distributions and variances obeying to (7), and then perform the inverse discrete curvelet transform what gives a field with the angular distribution of H exponents that was introduced in the curvelet space. The inverse curvelet transform stage of our synthesis method can be performed by fast discrete algorithms [Candes et al.(2006)Candes, Demanet, Donoho, and Ying]. The generated fractal surfaces have spectral densities following a orientation-dependent power-law, in a way that resembles the basic discrete curvelet tiling.

Acknowledgments

The author wish to dedicate this work to the memory of prof. Liacir dos Santos Lucena, and gratefully acknowledge the support of the Universidade Federal do Rio Grande do Norte (UFRN) and Universidade Federal Rural do Semi-Árido (UFERSA).

References

- [Mandelbrot and Van Ness(1968)] Benoit B Mandelbrot and John W Van Ness. Fractional brownian motions, fractional noises and applications. *SIAM review*, 10(4):422–437, 1968.
- [Hewett(1986)] TA Hewett. Fractal distributions of reservoir heterogeneity and their influence on fluid transport. In *SPE Annual Technical Conference and Exhibition*. OnePetro, 1986.
- [Sahimi and Tajar(2005)] Muhammad Sahimi and S Ehsan Tajar. Self-affine fractal distributions of the bulk density, elastic moduli, and seismic wave velocities of rock. *Physical Review E*, 71(4):046301, 2005.
- [Dashtian et al.(2011)Dashtian, Jafari, Sahimi, and Masihi] Hassan Dashtian, G Reza Jafari, Muhammad Sahimi, and Mohsen Masihi. Scaling, multifractality, and long-range correlations in well log data of large-scale porous media. *Physica A: Statistical Mechanics and its Applications*, 390(11):2096–2111, 2011.
- [Hardy and Beier(1994)] HH Hardy and Richard A Beier. *Fractals in reservoir engineering*. World Scientific, 1994.
- [Hansen et al.(2011)Hansen, Lucena, and Da Silva] Alex Hansen, Liacir S Lucena, and Luciano R Da Silva. Spatial correlations in permeability distributions due to extreme dynamics restructuring of unconsolidated sandstone. *Physica A: Statistical Mechanics and its Applications*, 390(4):553–560, 2011.

- [Sahini and Sahimi(1994)] von M Sahini and Muhammadpr Sahimi. *Applications of percolation theory*. CRC Press, 1994.
- [Dullien(2012)] Francis AL Dullien. *Porous media: fluid transport and pore structure*. Academic press, 2012.
- [Makse et al.(1995)]Makse, Davies, Havlin, Ivanov, King, and Stanley] Hernán A Makse, Glenn W Davies, Shlomo Havlin, Plamen Ch Ivanov, Peter R King, and H Eugene Stanley. Quantitative characterization of permeability fluctuations in sandstone. *arXiv preprint cond-mat/9512025*, 1995.
- [Ponson et al.(2006)]Ponson, Bonamy, Auradou, Mourot, Morel, Bouchaud, Guillot, and Hulin] Laurent Ponson, Daniel Bonamy, Harold Auradou, Guillaume Mourot, Stéphane Morel, Elisabeth Bouchaud, Claude Guillot, and Jean-Pierre Hulin. Anisotropic self-affine properties of experimental fracture surfaces. *International Journal of fracture*, 140(1):27–37, 2006.
- [Jennane et al.(2001)]Jennane, Ohley, Majumdar, and Lemineur] Rachid Jennane, William J Ohley, Sharmila Majumdar, and Gérald Lemineur. Fractal analysis of bone x-ray tomographic microscopy projections. *IEEE transactions on medical imaging*, 20(5):443–449, 2001.
- [Kamont(1995)] Anna Kamont. On the fractional anisotropic wiener field. *Probability and Mathematical Statistics-PWN*, 16(1):85–98, 1995.
- [Bonami and Estrade(2003)] Aline Bonami and Anne Estrade. Anisotropic analysis of some gaussian models. *Journal of Fourier analysis and applications*, 9(3):215–236, 2003.
- [Tavares and Lucena(2003)] DM Tavares and LS Lucena. Models for correlated multifractal hypersurfaces. *Physical Review E*, 67(3):036702, 2003.
- [Heneghan et al.(1996)]Heneghan, Lowen, and Teich] C Heneghan, SB Lowen, and Malvin C Teich. Two-dimensional fractional brownian motion: wavelet analysis and synthesis. In *Proceeding of Southwest Symposium on Image Analysis and Interpretation*, pages 213–217. IEEE, 1996.
- [Biermé and Richard(2008)] Hermine Biermé and Frédéric Richard. Estimation of anisotropic gaussian fields through radon transform. *ESAIM: Probability and Statistics*, 12:30–50, 2008.
- [Xiao(2009)] Yimin Xiao. Sample path properties of anisotropic gaussian random fields. In *A minicourse on stochastic partial differential equations*, pages 145–212. Springer, 2009.
- [Candes and Donoho(2000)] Emmanuel J Candes and David L Donoho. Curvelets: A surprisingly effective nonadaptive representation for objects with edges. Technical report, Stanford Univ Ca Dept of Statistics, 2000.
- [Starck et al.(2002)]Starck, Candès, and Donoho] Jean-Luc Starck, Emmanuel J Candès, and David L Donoho. The curvelet transform for image denoising. *IEEE Transactions on image processing*, 11(6):670–684, 2002.
- [Candès and Donoho(2004)] Emmanuel J Candès and David L Donoho. New tight frames of curvelets and optimal representations of objects with piecewise c_2 singularities. *Communications on Pure and Applied Mathematics: A Journal Issued by the Courant Institute of Mathematical Sciences*, 57(2):219–266, 2004.
- [Stephane(1999)] Mallat Stephane. A wavelet tour of signal processing, 1999.
- [Candes et al.(2006)]Candes, Demanet, Donoho, and Ying] Emmanuel Candes, Laurent Demanet, David Donoho, and Lexing Ying. Fast discrete curvelet transforms. *multiscale modeling & simulation*, 5(3):861–899, 2006.
- [Candes and Donoho(2005)] Emmanuel J Candes and David L Donoho. Continuous curvelet transform: I. resolution of the wavefront set. *Applied and Computational Harmonic Analysis*, 19(2):162–197, 2005.
- [Keys(1981)] Robert Keys. Cubic convolution interpolation for digital image processing. *IEEE transactions on acoustics, speech, and signal processing*, 29(6):1153–1160, 1981.
- [Peng et al.(1994)]Peng, Buldyrev, Havlin, Simons, Stanley, and Goldberger] C-K Peng, Sergey V Buldyrev, Shlomo Havlin, Michael Simons, H Eugene Stanley, and Ary L Goldberger. Mosaic organization of dna nucleotides. *Physical review e*, 49(2):1685, 1994.
- [Taquu et al.(1995)]Taquu, Teverovsky, and Willinger] Murad S Taquu, Vadim Teverovsky, and Walter Willinger. Estimators for long-range dependence: an empirical study. *Fractals*, 3(04):785–798, 1995.